Inorg. Chem. **1994**, *33*, 3169-3176

Structural Characterization of a Trinuclear Complex of Platinum(II) Containing Bridging 1-Methylcytosine Ligands. A Combined X-ray and Multinuclear NMR Study

Luisa Schenetti,[†] Giuliano Bandoli,[‡] Alessandro Dolmella,[‡] Guendalina Trovó,[§] and Bruno Longato[*],[§]

Dipartimento di Chimica, Universitá di Modena, Via Campi 183, 41100 Modena, Italy,
Centro di Studio sulla Stabilitá e Reattivitá dei Composti di Coordinazione, CNR, c/o
Dipartimento di Chimica Inorganica, Metallorganica ed Analitica, Universitá di Padova,
Via Marzolo 1, 35131 Padova, Italy, and Dipartimento di Scienze Farmaceutiche,
Universitá di Padova, Via Marzolo 5, 35131 Padova, Italy

Received October 6, 1993[⊗]

The dinuclear complexes *cis*-$[(PMe_3)_2Pt(1\text{-}MeCy(\text{-}H))]_2X_2$ (X = NO_3^- (**1A**), ClO_4^- (**1B**)), containing NH_2-deprotonated 1-methylcytosine (1-MeCy(-H)) ligands, in aqueous or DMSO solution, at 80 °C convert quantitatively into the corresponding trinuclear derivatives *cis*-$[(PMe_3)_2Pt(1\text{-}MeCy(\text{-}H))]_3X_3$ (**2A,B**) which have been characterized in the solid state by single-crystal X-ray analysis and in solution by multinuclear (^1H, ^{31}P, ^{195}Pt, ^{13}C, and ^{15}N) NMR spectroscopy. The nitrate salt (**2A**) crystallizes from ethanol in the triclinic system, space group $P\bar{1}$. The crystals, stable only in the presence of the solvent, have the following cell dimensions: $a = 13.542(5)$ Å, $b = 17.352(5)$ Å, $c = 20.721(6)$ Å, $\alpha = 113.13(2)°$, $\beta = 104.30(3)°$, $\gamma = 95.77(3)°$, Z = 2. The structure, formulated as *cis*-$[(PMe_3)_2Pt(1\text{-}MeCy(\text{-}H))]_3(NO_3)_3\cdot EtOH\cdot H_2O$, was refined to $R = 6.3$ and $R_w = 6.3$. Better structural data were obtained with the perchlorate derivative (**2B**), *cis*-$[(PMe_3)_2Pt(1\text{-}MeCy(\text{-}H))]_3(ClO_4)_3\cdot 2H_2O$, whose structure was refined to $R = 4.4$ and $R_w = 4.9$. The colorless prisms formed from aqueous solutions have the following crystallographic data: triclinic system, space group $P\bar{1}$, $a = 14.634(7)$ Å, $b = 14.791(9)$ Å, $c = 14.980(9)$ Å, $\alpha = 101.93(5)°$, $\beta = 103.46(5)°$, $\gamma = 90.50(4)°$, Z = 2. In both salts, the molecular structure of the cationic complex contains three *cis*-$(PMe_3)_2Pt$ units linked to three 1-methylcytosine anions through the N(3) and N(4) atoms. The resulting 12-membered ring contains the pyrimidinic rings almost perpendicular to the plane defined by the metal atoms. Each platinum has a square-planar coordination with a Pt···Pt distance of 5.2 Å. The ^1H, ^{31}P, and ^{13}C NMR spectra indicate that the approximate S_3 symmetry of the cation is maintained in solution. The compounds **1A** and **2A** were also characterized by ^{15}N NMR spectroscopy, at natural abundance. The spectroscopic data, obtained in DMSO-d_6 solution, are compared with those of the derivative *cis*-$[(PMe_3)_2Pt(1\text{-}MeCy)_2](NO_3)_2$ containing as ligands the *neutral* N(3)-bonded nucleobase. The dinuclear and trinuclear complexes exhibit very similar ^{15}N chemical shifts and $^2J_{PN}$ coupling constants but remarkably different from those of the mononuclear complex.

Introduction

The binding modes of the nucleobases toward metal centers have been investigated in detail in the last two decades and many complexes of these nucleic acid components, in particular with platinum(II) and -(IV), have been structurally characterized. With the model nucleobase 1-methylcytosine (1-MeCy), the coordination of the metal center occurs generally at the N(3) atom of the pyrimidine ring.[1] It has been shown that metal binding determines an increase in acidity of the exocyclic NH_2 hydrogens of the nucleobase, as indicated by the downfield shift of the resonance of these protons in the NMR spectra of complexes containing N(3)-coordinated 1-MeCy.[2] The concomitant presence of a hydroxo ligand on the coordination sphere of the metal causes an intramolecular condensation reaction with the consequent deprotonation of the nucleobase. Thus, mononuclear[3] and binuclear[4] complexes of platinum(II) and -(IV) containing NH_2-deprotonated 1-methylcytosine have been characterized (complexes **I**–**III** of Chart 1).

Interestingly, whereas the dinuclear species **III** appears to be stable, the mononuclear complex **II**, containing the N(3),N(4) chelated nucleobase, in aqueous solution undergoes hydrolysis with formation of the stable species **IV** in which the cytosine adopts the rare iminooxo tautomeric form.

We have recently reported that a facile deprotonation of the exocyclic NH_2 group in 1-methylcytosine and 9-ethyladenine (9-EtAd) occurs when these nucleobases are reacted with the dinuclear hydroxo complex *cis*-$[(PMe_3)_2Pt(\mu\text{-}OH)]_2(NO_3)_2$. The resulting products are the dinuclear derivatives *cis*-$[(PMe_3)_2Pt(1\text{-}MeCy(\text{-}H))]_2(NO_3)_2$[5] and *cis*-$[(PMe_3)_2Pt(9\text{-}EtAd(\text{-}H))]_2(NO_3)_2$,[6] respectively, in which the bridging nucleobases adopt a head-to-tail arrangement, the same as the one found in the amine analogue (complex **III** of Chart 1). We noticed that the cytosine complex, in aqueous or DMSO solution, slowly converts into a thermodynamically more stable species for which preliminary spectroscopic data suggested the formation of the corresponding *mononuclear* derivative, *cis*-$[(PMe_3)_2Pt(1\text{-}MeCy(\text{-}H))]^+$, with the nucleobase acting as chelated ligand through the N(3),N(4)-atoms.[5] This complex has now been isolated as nitrate (**2A**) and perchlorate (**2B**) salts and characterized in the solid state by single-crystal X-ray analysis and in solution by multinuclear (^1H, ^{31}P, ^{13}C, ^{195}Pt, and natural-abundance ^{15}N) NMR spectroscopy. In this paper we present the results of this

---

[*] Author to whom correspondence should be addressed.

[†] Dipartimento di Chimica, Universitá di Modena.

[‡] Dipartimento di Scienze Farmaceutiche, Universitá di Padova.

[§] CNR.

[⊗] Abstract published in *Advance ACS Abstracts*, May 15, 1994.

(1) Lippert, B. *Prog. Inorg. Chem.* **1989**, *37*, 1.

(2) (a) Graves, B. J.; Hodgson, D. J. *J. Am. Chem. Soc.* **1979**, *101*, 5608. (b) Orbell, J.D.; Marzilli, L. G.; Kistenmacher, T. J. *J. Am. Chem. Soc.* **1981**, *103*, 5126. (c) Faggiani, R.; Lippert, B.; Lock, C. J. L. *Inorg. Chem.* **1982**, *21*, 3210. (d) Lippert, B.; Thewalt, U.; Schöllhorn, H.; Goodgame, D. M. L.; Rollins, R. W. *Inorg. Chem.* **1984**, *23*, 2807. (e) Trovó, G.; Longato, B. *Inorg. Chim. Acta* **1992**, *192*, 13.

(3) Schöllhorn, H.; Beyerle-Pfnür, R.; Thewalt, U.; Lippert, B. *J. Am. Chem. Soc.* **1986**, *108*, 3680.

(4) (a) Lippert, B.; Schöllhorn, B.; Thewalt, U. *J. Am. Chem. Soc.* **1986**, *108*, 6616. (b) Faggiani, R.; Lippert, B.; Lock, C. J. L.; Speranzini, R. A. *J. Am. Chem. Soc.* **1981**, *103*, 1111.

(5) Trovó, G.; Bandoli, G.; Casellato, U.; Corain, B.; Nicolini, M.; Longato, B. *Inorg. Chem.* **1990**, *29*, 4616.

(6) Trovó, G.; Bandoli, G.; Nicolini, M.; Longato, B. *Inorg. Chim. Acta* **1993**, *211*, 95.

Chart 1

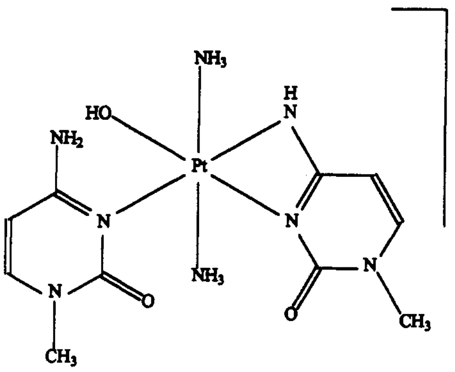

I

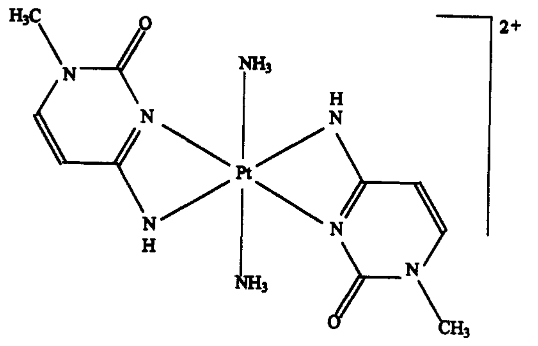

II

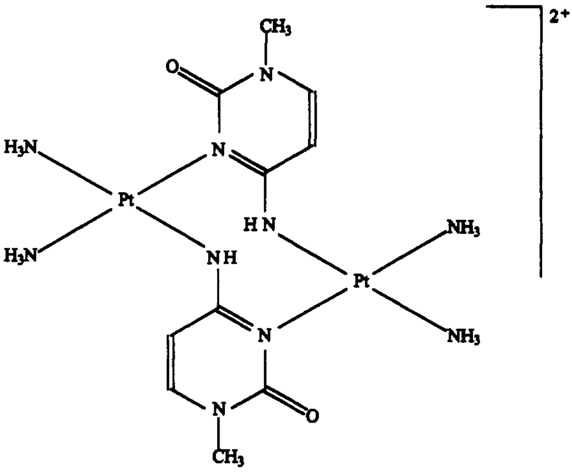

III

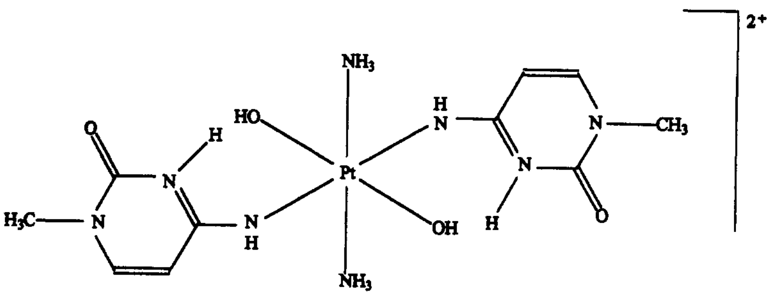

IV

investigation showing that, in fact, the new products contain the *trinuclear* complex *cis*-[(PMe$_3$)$_2$Pt(1-MeCy(-H))]$_3^{3+}$, in which the nucleobase symmetrically bridges three metal centers. The structural and spectroscopic data are compared with those of the dinuclear derivative *cis*-[(PMe$_3$)$_2$Pt(1-MeCy(-H))]$_2^{2+}$ (1) and those of the mononuclear complex *cis*-[(PMe$_3$)$_2$Pt(1-MeCy)$_2$]$^{2+}$ containing the same nucleobase as the *neutral* ligand.[7]

Nucleobase–metal complexes forming *cyclic* trimers are rare.[8] The present work appears to be the first report of a triplatinum–cytosine complex.

Experimental Section

Materials and Methods. The platinum complexes *cis*-[(PMe$_3$)$_2$Pt(μ-OH)]$_2$(NO$_3$)$_2$, *cis*-[(PMe$_3$)$_2$Pt(1-MeCy(-H))]$_2$(NO$_3$)$_2$, and *cis*-[(PMe$_3$)$_2$Pt(1-MeCy)$_2$](NO$_3$)$_2$ were synthesized as previously reported.[5,7] The complex *cis*-[(PMe$_3$)$_2$Pt(μ-OH)]$_2$(ClO$_4$)$_2$ was obtained by treating an aqueous solution of *cis*-[(PMe$_3$)$_2$Pt(μ-OH)]$_2$(NO$_3$)$_2$ with a stoichiometric amount of NaClO$_4$. The perchlorate salt precipitated in quantitative yield, being virtually insoluble in water.

Safety Note. This salt is *unpredictably* explosive. Only small amounts of material should be prepared, and these should be handled with great caution. 1-Methylcytosine was purchased from Sigma Chemical Co.

The ^{1}H, ^{13}C, ^{31}P, ^{195}Pt, and ^{15}N NMR spectra were obtained in D$_2$O and/or DMSO-d_6 at 298 K in 10-mm sample tubes on a Bruker 400AMX-WB spectrometer operating at 400.13, 100.61, 161.98, 85.88, and 40.56 MHz, respectively. The external references are H$_3$PO$_4$ (85% w/w in D$_2$O) for ^{31}P, Na$_2$PtCl$_4$ in D$_2$O (adjusted to −1628 ppm from Na$_2$PtCl$_6$) for ^{195}Pt, and CH$_3$NO$_2$ (in CDCl$_3$ at 50% w/w) for ^{15}N. ^{1}H and ^{13}C chemical shifts are referred to internal TMS or the sodium salt of 3-(trimethylsilyl)-[2,2,3,3-$^2H_4$]propionic acid. For proton-decoupled ^{13}C, ^{31}P, and ^{195}Pt spectra, typical conditions were as follows: 0.8–1 s for relaxation delay, 60° pulse angle, spectral widths of 18 kHz, 12 kHz, and 50 kHz, respectively, with 16 or 32K data points. Natural-abundance ^{15}N NMR spectra were obtained using a different procedure including refocused INEPT and heterocorrelated HMQC-COSY experiments[9] for protonated nitrogen[10] and a modified INEPT for nonprotonated nitrogen atoms.[11]

For the INEPT experiments the acquisition parameters were the following: spectral width of 20 kHz with 32K data points, a relaxation delay of 1–2 s and number of scans 5000–10 000, ^{1}H P_w(90°) = 22 μs, ^{15}N P_w(90°) = 17 μs. The delay for the coherence transfer was selected corresponding to a $^1J_{NH}$ of 90 Hz (for refocused INEPT) and a long range of 8 Hz (for modified INEPT).

The shift correlation spectra of *cis*-[(PMe$_3$)$_2$Pt(1-MeCy)$_2$](NO$_3$)$_2$ and *cis*-[(PMe$_3$)$_2$Pt(1-MeCy(-H))]$_2$(NO$_3$)$_2$ were obtained through 2D inverse experiments. The acquisition parameters were the following: spectral width in F$_2$ was 2.64 ppm with a FIDRES of 2.35 Hz, and number of scans 256; in F$_1$ the spectral width was 200 ppm with a FIDRES of 31.68 Hz and a number of increments 256. A delay of 5.5 ms was selected in order to allow the evolution of $^1J_{N-H}$ (typically 90 Hz).

In order to obtain the heteronuclear couplings, most of the ^{1}H, ^{31}P, ^{13}C, and ^{195}Pt NMR spectra were also obtained on a JEOL 90Q spectrometer.

Synthesis of *cis*-[(PMe$_3$)$_2$Pt(1-MeCy(-H))]$_3$(NO$_3$)$_3$ (2A). A solution of *cis*-[(PMe$_3$)$_2$Pt(μ-OH)]$_2$(NO$_3$)$_2$ (1.20 g; 1.41 mmol) and 1-methylcytosine (0.353 g; 2.82 mmol) in 50 mL of H$_2$O was stirred at room temperature for 48 h and then warmed at 80 °C for 6 days. The ^{31}P NMR spectrum of the resulting solution showed the presence of the title compound and a residual amount of *cis*-[(PMe$_3$)$_2$Pt(1-MeCy(-H))]$_2$-

---

(7) Trovò, G.; Valle, G.; Longato, B. *J. Chem. Soc., Dalton Trans.* **1993**, 669.

(8) Smith, D. P.; Baralt, E.; Morales, B.; Olmstead, R. M.; Maestre, M. F.; Fish, R. H. *J. Am. Chem. Soc.* **1992**, *114*, 10647.

(9) (a) Morris, G. A.; Freeman, R. *J. Am. Chem. Soc.* **1979**, *101*, 760. (b) Shaka, A.J.; Barker, P. B.; Freman, R. *J. Magn. Reson.* **1985**, *64*, 547.

(10) (a) Bax, A.; Griffey, R. H.; Hawkins, B. L. *J. Magn. Reson.* **1983**, *55*, 301. (b) Bax, A.; Subramanian, S. *J. Magn. Reson.* **1986**, *67*, 565.

(11) Glemarec, C.; Remaud, G.; Chattopadhyaya, J. *Magn. Reson. Chem.* **1988**, *26*, 307.

Table 1. Crystallograhic Data for *cis*-$[(PMe_3)_2Pt(1\text{-}MeCy(\text{-}H))]_3X_3$ ($X = NO_3^-$ (**2A**), ClO_4^- (**2B**))

	$X = NO_3^-$, **2A**·EtOH·H_2O	$X = ClO_4^-$, **2B**·2H_2O
chem formula	$C_{35}H_{80}N_{12}O_{14}P_6Pt_3$	$C_{33}H_{76}N_9O_{17}Cl_3P_6Pt_3$
fw	1663.8	1748.5
cryst system	triclinic	triclinic
space group	$P\bar{1}$	$P\bar{1}$
a, Å	13.542(5)	14.634(7)
b, Å	17.352(5)	14.791(9)
c, Å	20.721(6)	14.980(9)
α, deg	113.13(2)	101.93(5)
β, deg	104.30(3)	103.46(5)
γ, deg	95.77(3)	90.50(4)
V, Å^3	4230.9(2.6)	3079.8(3.1)
Z	2	2
λ, Å (Mo Kα)	0.710 73	0.710 73
D_{calcd}, g cm^{-3}	1.306	1.885
μ, cm^{-1}	50.9	71.5
I_{max}/I_{min}		1.0/0.35
T, °C	21	21
obsd reflcns	5152	5767
resid, %: R, R_w[a]	6.3, 6.3	4.4, 4.9
goodness-of-fit		1.05

[a] $R = \sum|\Delta|/\sum|F_o|$; $R_w = (\sum w|\Delta|^2/\sum w|F_o|^2)^{1/2}$.

$(NO_3)_2$ (**1A**) (*ca.* 7%). The solvent was evaporated under vacuum, and the residue was dissolved in hot ethanol (50 mL) and then left to crystallize. The colorless crystals, formed in 2 days at room temperature, were separated by filtration and dried under vacuum (*ca.* 10^{-3} Torr, 48 h) to a constant weight. During this time the crystals become an amorphous powder (0.7 g; yield 55%). Anal. Calc for $C_{11}H_{24}N_4O_4P_2Pt$: C, 24.77; H, 4.53; N, 10.50. Found: C, 24.29; H, 4.46; N, 10.48. ^1H NMR in DMSO-d_6 at 27 °C (δ, ppm): 7.44 (d, $^3J_{HH}$ 7.5 Hz, 1 H, H(6)); 6.46 (broad singlet, 1 H, N(4)H); 6.05(dd, $^3J_{HH}$ 7.5 and $^5J_{PH}$ 1.8 Hz, with unresolved ^{195}Pt satellites, 1 H, H(5)); 3.19 (s, 3 H, N(1)CH_3); 1.72(d with ^{195}Pt satellites, $^2J_{HP}$ 11.6 Hz, $^3J_{HPt}$ 34.2 Hz, 9 H, PMe_3); 1.54 (d with ^{195}Pt satellites, $^2J_{HP}$ 11.05 Hz, $^3J_{HPt}$ 32.2 Hz, 9 H, PMe_3). ^1H NMR in CD_3NO_2 at 24 °C (δ, ppm): 7.14 (d, $^3J_{HH}$ 7.3 Hz, 1 H, H(6)); 6.6 (broad singlet, 1 H, N(4)H); 6.23(dd, $^3J_{HH}$ 7.3 and $^5J_{PH}$ 1.7 Hz, with unresolved ^{195}Pt satellites, 1 H, H(5)); 3.25 (s, 3 H, N(1)CH_3); 1.81 (d with ^{195}Pt satellites, $^2J_{HP}$ 11.2 Hz, $^3J_{HPt}$ 34.2 Hz, 9 H, PMe_3); 1.62 (d, $^2J_{HP}$ 10.7 Hz, $^3J_{HPt}$ 32.2 Hz, 9 H, PMe_3).

Synthesis of *cis*-$[(PMe_3)_2Pt(1\text{-}MeCy(\text{-}H))]_3(ClO_4)_3$ (2B). A suspension of *cis*-$[(PMe_3)_2Pt(\mu\text{-}OH)]_2(ClO_4)_2$ (253.5 mg, 0.273 mmol) and 1-methylcytosine (68.3 mg; 0.546 mmol) in 10 mL of H_2O was stirred at ambient temperature for 48 h and then warmed at 80 °C for 3 days. The resulting mixture was cooled at room temperature and the obtained white solid filtered out, washed with cold water, and dried under vacuum (10^{-3} Torr) at 50 °C for 12 h. The yield of pure, anhydrous, complex was virtually quantitative. Anal. Calc for $C_{11}H_{24}N_3O_5P_2ClPt$: C, 23.14; H, 4.24; N, 7.36. Found: C, 22.88; H, 4.23; N, 7.38. ^1H NMR in DMSO-d_6 at 27 °C (δ, ppm): 7.66 (d, $^3J_{HH}$ 7.6 Hz, 1 H, H(6)); 6.00 (dd, $^3J_{HH}$ 7.3 and $^5J_{PH}$ 1.7 Hz, with unresolved ^{195}Pt satellites, 1 H, H(5); 5.81 (broad singlet, 1 H, N(4)H); 3.19 (s, 3 H, N(1)CH_3); 1.70 (d with ^{195}Pt satellites, $^2J_{HP}$ 11.4 Hz, $^3J_{HPt}$ 33 Hz, 9 H, PMe_3); 1.51 (d, $^2J_{HP}$ 10.5 Hz, $^3J_{HPt}$ 33.3 Hz, 9 H, PMe_3). ^{31}P NMR spectrum in DMSO at 27 °C (δ, ppm): −27.91 ($^2J_{PP}$ 25.0, $^1J_{PPt}$ 3233.7 Hz), −28.97 ($^2J_{PP}$ 25.0, $^1J_{PPt}$ 3110.4 Hz).

Crystallography. Suitable crystals of **2A**, analyzing as *cis*-$[(PMe_3)_2Pt(1\text{-}MeCy(\text{-}H))]_3(NO_3)_3$·EtOH·$H_2O$ (**2A**·EtOH·H_2O) were obtained by cooling a saturated solution of the complex in ethanol, from 70 °C to room temperature, operating in a closed flask. Since they were unstable in the absence of the mother liquor, a crystal was rapidly inserted into a capillary containing a drop of mother solution and then sealed. The data were collected on a colorless transparent crystal having the dimensions of 0.50 × 0.12 × 0.20 mm^3, at room temperature, on a Siemens Nicolet R3m/V four-circle automated diffractometer, up to $2\theta = 45°$. Characteristics of the data collection, processing, and refinement are given in Table 1. Heavy-atom parameters were found from Patterson synthesis, and the non-H atoms were located in subsequent difference Fourier syntheses. As is frequently the case, in **2A** the two nitrate groups are severely disordered and the ethanol and water molecules are suffering from high thermal motion. The relatively small amount of high-angle data, the high thermal motion also in the "inner core" of the complex, the high disorder at NO_3^-, EtOH, and H_2O units, and a moderate deterioration of the crystal during the data collection, as pointed out by the intensities of two standard reflections monitored every 200 reflections,

Table 2. Atomic Coordinates (×10^4) and Equivalent Isotropic Displacement Coefficients (Å^2 × 10^3) for **2B**·2H_2O

	x	y	z	U[a]
Pt(1)	90(1)	2622(1)	2007(1)	42(1)
Pt(2)	−2651(1)	1730(1)	3594(1)	41(1)
Pt(3)	−3480(1)	3228(1)	664(1)	44(1)
P(1)	284(3)	2416(3)	525(3)	61(2)
P(2)	1353(3)	1834(3)	2540(3)	59(2)
P(3)	−3963(3)	1314(3)	4004(3)	56(2)
P(4)	−1986(3)	363(3)	3648(3)	58(2)
P(5)	−3512(3)	3534(3)	−766(3)	59(2)
P(6)	−4790(3)	2276(3)	181(3)	62(2)
C(7)	−415(19)	1455(18)	−272(18)	127(8)
C(8)	11(15)	3447(15)	93(15)	99(6)
C(9)	1489(18)	2298(17)	336(17)	118(8)
C(10)	1258(15)	647(14)	1881(14)	90(6)
C(11)	1514(12)	1665(12)	3718(12)	72(4)
C(12)	2532(17)	2257(16)	2553(17)	114(7)
C(13)	−3804(13)	1282(12)	5245(12)	77(5)
C(14)	−4534(15)	195(14)	3341(14)	91(6)
C(15)	−4917(12)	2085(11)	3805(12)	70(4)
C(16)	−2028(13)	−169(12)	4643(13)	82(5)
C(17)	−2365(15)	−544(14)	2610(15)	99(6)
C(18)	−707(15)	476(14)	3808(14)	92(6)
C(19)	−2646(14)	4432(13)	−756(13)	82(5)
C(20)	−4594(14)	3996(13)	−1342(13)	87(5)
C(21)	−3281(15)	2546(14)	−1621(14)	91(6)
C(22)	−4858(14)	1468(14)	947(14)	88(6)
C(23)	−5059(16)	1472(15)	−953(16)	104(7)
C(24)	−5812(17)	2925(16)	241(16)	109(7)
O(2)	1262(7)	3958(7)	3680(7)	67(4)
O(2a)	−2949(8)	3297(7)	5153(7)	64(4)
O(2b)	−3408(8)	5324(6)	1104(7)	66(4)
N(1)	609(8)	3959(8)	4891(8)	53(5)
N(1a)	−3566(9)	4466(8)	4441(9)	58(5)
N(1b)	−1897(9)	5824(8)	1826(9)	61(5)
N(3)	−87(7)	3070(7)	3388(7)	41(4)
N(3a)	−3129(8)	3081(7)	3590(8)	48(5)
N(3b)	−2357(7)	4220(7)	1293(8)	44(4)
N(4)	−1487(7)	2185(7)	3176(7)	42(4)
N(4a)	−3306(7)	2889(7)	1982(7)	45(4)
N(4b)	−1200(8)	3147(7)	1514(8)	46(4)
C(1)	1449(11)	4525(12)	5536(11)	73(7)
C(1a)	−3636(13)	5030(12)	5380(11)	78(7)
C(1b)	−2196(13)	6802(11)	1952(14)	78(8)
C(2)	620(10)	3680(10)	3984(10)	52(6)
C(2a)	−3194(10)	3599(10)	4442(11)	51(6)
C(2b)	−2576(10)	5130(10)	1395(10)	50(6)
C(4)	−820(9)	2771(8)	3718(9)	41(5)
C(4a)	−3394(9)	3397(9)	2742(9)	41(5)
C(4b)	−1421(9)	4010(9)	1624(8)	42(5)
C(5)	−806(10)	3095(10)	4724(10)	54(6)
C(5a)	−3763(11)	4309(9)	2812(11)	58(6)
C(5b)	−716(11)	4744(10)	2055(10)	59(6)
C(6)	−78(12)	3661(11)	5249(10)	61(6)
C(6a)	−3835(11)	4800(10)	3640(11)	58(6)
C(6b)	−996(10)	5638(9)	2124(10)	50(6)
Cl(1)	2468(4)	9584(3)	9588(3)	83(2)
O(3)	2366(12)	8838(12)	8861(12)	135(6)
O(4)	2743(16)	9302(16)	10460(17)	182(8)
O(5)	3156(16)	10231(15)	9576(15)	172(8)
O(6)	1521(15)	10004(14)	9455(14)	160(7)
Cl(2)	550(5)	8180(4)	2979(4)	98(3)
O(7)	585(19)	7385(19)	2411(19)	219(10)
O(8)	1608(56)	8415(55)	3453(57)	280(32)
O(9)	−86(19)	8090(17)	3591(18)	195(9)
O(10)	283(49)	8982(40)	2584(40)	207(22)
O(8′)[b]	−293(25)	8358(24)	2242(24)	142(10)
O(9′)[b]	1212(41)	7966(38)	3807(38)	206(20)
O(10′)[b]	1144(34)	8941(29)	3001(30)	159(13)
Cl(3)	6116(3)	7582(3)	4013(3)	74(2)
O(11)	5926(15)	7821(14)	3147(15)	163(7)
O(12)	5353(13)	6966(12)	3973(12)	130(6)
O(13)	6163(10)	8400(9)	4700(10)	99(4)
O(14)	6987(15)	7142(14)	4165(15)	161(7)
Ow(1)	1851(11)	4364(11)	2133(11)	119(5)
Ow(2)	2172(15)	6231(14)	2970(14)	158(7)

[a] Equivalent isotropic U defined as one-third of the trace of the orthogonalized $\mathbf{U}_{ij}$ tensor. [b] Disordered atoms.

Table 3. $^{31}P\{^1H\}$ and $^{195}Pt\{^1H\}$ NMR Data for *cis*-$[(PMe_3)_2Pt(1\text{-}MeCy(\text{-}H))]_2(NO_3)_2$, **1A**, and *cis*-$[(PMe_3)_2Pt(1\text{-}MeCy(\text{-}H))]_3(NO_3)_3$, **2A**

compd	solvent	$\delta(^{31}P)$, ppm ($^2J_{PP}$, Hz)	$\delta(^{195}Pt)$, ppm	($^1J_{P-Pt}$, Hz)
1A	D_2O	−32.75, −33.03 (26.2)	−4211 (d, d)	(3135, 3293)
1A	DMSO-d_6	−31.91, −32.44 (26.2)	−4198[a] (d, d)	(3066, 3269)
2A	D_2O	−28.52, −30.41 (24.4)	−4369 (d, d)	(3264, 3121)
2A	DMSO-d_6	−27.77, −29.14 (24.4)	−4354[a] (d, d)	(3221, 3135)
2A	CD_3OD	−28.88, −30.35 (25.0)		(3259, 3120)

[a] The chemical shift value reported in ref 5 is uncorrect.

did not allow an accurate determination of the structure of **2A**; however, the stereochemistry of the cationic trimer was unambiguously determined. In addition, a fitting of the "inner core" of **2A** and its perchlorate analog **2B** shows such trimers to be substantially superimposable (Figure A of the supplementary material). Consequently, the discussion of all the relevant data, such as bond distances and angles, refers to the more accurate structure determination carried out on the perchlorate salt, **2B**. Suitable crystals, analyzing as $[(PMe_3)_2Pt(1\text{-}MeCy(\text{-}H))]_3(ClO_4)_3{\cdot}2H_2O$ (**2B**$\cdot 2H_2O$), were obtained by slow cooling of a saturated (at 80 °C) aqueous solution of the complex. The presence of H_2O in the crystal lattice was proved by thermogravimetric analysis which was carried out with a Perkin-Elmer TGS-2 themobalance, operating at a heating rate of 40 °C min^{-1}. A 1.91% decrease in weight was observed in the 36–179 °C temperature range. Crystallographic data are reported in Table 1, while other information related to data collection and refinement procedure have been deposited as supplementary material. The data were collected on a colorless transparent needle-shaped crystal (0.20 × 0.30 × 0.15 mm^3). An empirical absorption correction, based on seven reflections at $\chi \sim 270°$ for different azimuthal angles (ψ-scans), was made. Fractional atomic coordinates and thermal isotropic equivalent parameters for **2B**$\cdot 2H_2O$ are listed in Table 2. The SHELXTL-PLUS package of computer programs[12] was employed for the solution and refinement of the structures.

Results and Discussion

We have earlier shown that the hydroxo complex *cis*-$[(PMe_3)_2Pt(\mu\text{-}OH)]_2(NO_3)_2$ reacts with 2 equiv of 1-methylcytosine in aqueous solution at ambient conditions in a few hours.[5] The initial reaction product is the dinuclear complex *cis*-$[(PMe_3)_2Pt(1\text{-}MeCy(\text{-}H))]_2(NO_3)_2$, **1A**, which contains the NH_2-deprotonated cytosine ligands bridging two *cis*-$(PMe_3)_2Pt$ units through the N(3) and N(4) atoms. The complex, in H_2O or DMSO at 80 °C, converts into a thermodynamically more stable species, **2A**, which has been now isolated and characterized. The product, very soluble in water, is moderately soluble in hot ethanol from which it crystallizes as large colorless prisms. In the absence of mother liquor the crystals become immediately opaque, and in a few minutes they form a white powder whose elemental analysis and ^1H, ^{13}C, ^{31}P, and ^{195}Pt NMR spectra are consistent with the formulation $[(PMe_3)_2Pt(1\text{-}MeCy(\text{-}H))](NO_3)$. In the proton NMR spectrum (at 89.55 MHz) the H(5) and H(6) cytosine protons exhibit the usual AB multiplet (^3J *ca.* 7 Hz). The resonance attributable to H(5) shows, in addition, coupling with one of the phosphorus ligands ($^5J_{PH}$ *ca.* 2 Hz) and, although not completely resolved, with ^{195}Pt ($^4J_{PtP}$ *ca.* 9 Hz). As observed in the case of **1A**, the N(4)H proton in D_2O exchanges rapidly (a few minutes) with the solvent, but its resonance is detectable as a broad singlet in DMSO-d_6 (δ 6.46) or CD_3NO_2 (δ 6.6). The phosphine methyl protons exhibit two well-separated sets of resonances due to the presence of chemically unequivalent phosphine ligands. Accordingly, the ^{31}P NMR spectrum (at 36.23 MHz) of **2A** (Table 3) shows a AB quartet with $^2J_{PP} = 25$ Hz, a value typical for a *cis*-$(PMe_3)_2Pt$ arrangement. The multiplet is flanked by ^{195}Pt satellites due to one-bond platinum–phosphorus coupling but lacks the weak resonances, due to long-range ^{195}Pt–^{31}P interactions, observed in the spectrum of the parent complex **1A**.[5]

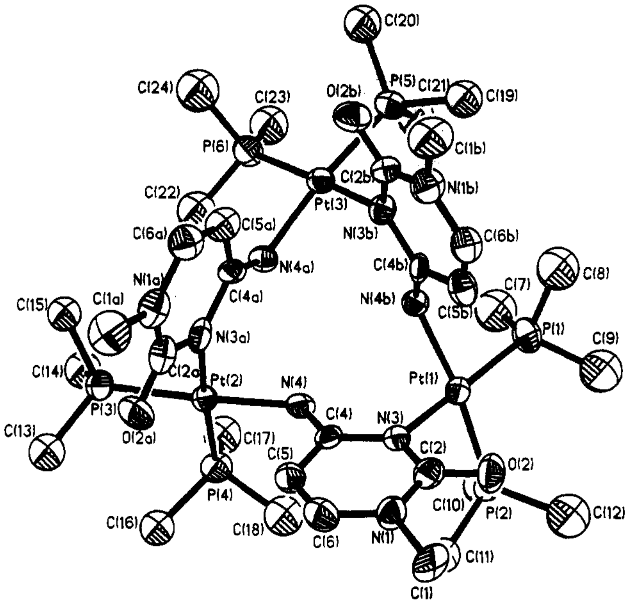

Figure 1. Perspective view of the cation *cis*-$[(PMe_3)_2Pt(1\text{-}MeCy(\text{-}H))]_3^{3+}$ in **2B**$\cdot 2H_2O$, showing the atom-numbering scheme. The three ClO_4^- counteranions and the two water molecules are omitted for clarity.

As shown in Table 3, the chemical shift differences of the two phosphines in **2A** ($\Delta\delta = 1.89$ ppm in D_2O) and in **1A** (0.28 ppm) are remarkably different, but the values of their $^1J_{PtP}$ constants are very similar indicating that the donor atoms *trans* to the PMe_3 ligands are the same in the two compounds.[13]

In line with these observations are the data obtained from the ^{195}Pt and ^{13}C NMR spectra. The proton-decoupled ^{195}Pt NMR spectrum of **2A** shows the presence of a single set of resonances, a doublet of doublets whose separation compares well with the values of $^1J_{Pt-P}$ obtained from the corresponding ^{31}P NMR spectrum. The multiplet, centered at δ −4369, appears shifted 158 ppm upfield with respect to the value found for the dinuclear derivative (see Table 3). On consideration of the large variation of ^{195}Pt chemical shifts in platinum(II) complexes,[14] the relatively small changes of this parameter observed in **1A** and **2A** are still in agreement with the suggestion that the ligand set around the metal center in the two complexes is the same.

The ^{13}C NMR spectrum of **2A**, obtained in DMSO-d_6 and CD_3OD, displays a single set of resonances for each carbon atom of the nucleobase, as shown in Table 4. Most of these resonances, depending on the solvent used, occur as doublets owing to the coupling with one of the phosphine ligands, and this coupling effect is seen also for the exocyclic $N(1)CH_3$ resonance ($^5J_{C-P}$ *ca.* 4 Hz). Moreover the spectrum obtained at 22.43 MHz exhibits the C(2), C(4), and C(5) resonances flanked by ^{195}Pt satellites, which, however, appear well-resolved only in CD_3OD solution.

At lower field intensity the phosphine methyl resonances are seen as a complex pattern, flanked by the ^{195}Pt satellites, as result of the chemical unequivalence of the two PMe_3 ligands. In the spectra obtained at 100.61 MHz two well-separated sets of first-order doublet of doublets are observed attributable to the one- and three-bond ^{13}C–^{31}P couplings. The parent complex **1A** exhibits a quite similar pattern, but unlike **2A**, all the pyrimidinic carbon resonances occur as singlets. The comparision of the ^{13}C parameters, collected in Table 4, shows that the rearrangement of the dinuclear species causes small changes for all the resonances, with the exception of that attributed to C(4), which appears remarkably upfield shifted (5.66 ppm) in the thermodynamic product.

---

(12) Sheldrick, G. M. SHELXTL-PLUS: An Integrated System for Solving, Refining and Displaying Crystal Structures from Diffraction Data. University of Gottingen, Germany, 1987.

(13) (a) Pregosin, P. S.; Kunz, R. W. In *³¹P and ¹³C NMR of Transition Metal Phosphine Complexes*; Dieh, P., Fluck, E., Kodfeld, R., Eds.; Springer-Verlag: Berlin, 1979; p 67. (b) Bandoli, G.; Trovó, G.; Dolmella, A.; Longato, B. *Inorg. Chem.* **1992**, *31*, 45.

(14) Pregosin, P. S. *Coord. Chem. Rev.* **1982**, *33*, 512.

Table 4. ^{13}C{^{1}H} NMR Data for *cis*-[(PMe$_3$)$_2$Pt(1-MeCy(-H))]$_2$(NO$_3$)$_2$, **1A**, and *cis*-[(PMe$_3$)$_2$Pt(1-MeCy(-H))]$_3$(NO$_3$)$_3$, **2A**

compd	solvent	cytosine resonances, ppm (J, Hz) N(CH$_3$) ($^5J_{C-P}$)	C$_2$ ($^3J_{C-P}$)	C$_4$ ($^3J_{C-P}$)	C$_5$ ($^4J_{C-P}$)	C$_6$ ($^5J_{C-P}$)	phosphine resonance, ppm (J, Hz) P(CH$_3$)$_3$ ($^1J_{C-P}$; $^3J_{C-P}$; $^2J_{C-Pt}$)
1A	DMSO-d_6	36.81^a (d, 4.5)	154.50	169.88	99.34	142.07	15.50 (d, d) (41.7; 6.2; 44), 15.10 (d, d) (40.8; 4.3; 43)
2A	DMSO-d_6	37.13 (d, 4.3)	155.22 (d, *ca.* 1)	164.22 (d, 4.7)	97.8 (d, 0.9)	143.97	14.00 (d, d) (42.0; 6.1; 44), 14.9 (d, d) (41; 4.7; 43)
2A	CD$_3$OD	37.75^a	157.11^a (d, 1.2)	162.14^b (d, 3.6)	99.82^c (d, 2.9)	145.02	17.3–12.8 (complex multiplet)

^{a} J_{C-Pt} *ca.* 4.8 Hz. ^{b} J_{C-Pt} *ca.* 20 Hz. ^{c} Unresolved ^{195}Pt satellites.

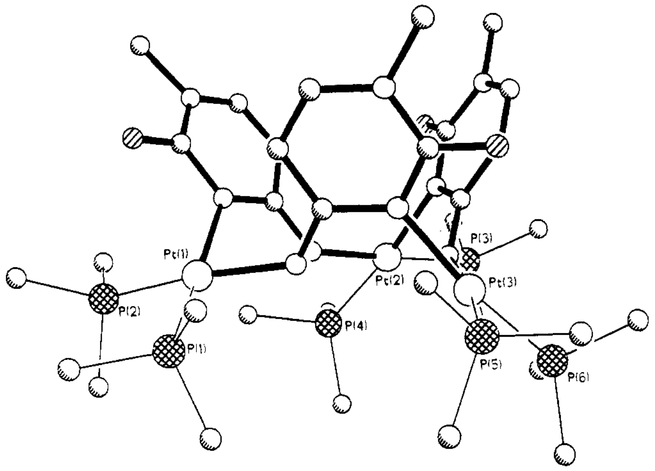

Figure 2. View of the cytosine rings in the *cis*-[(PMe$_3$)$_2$Pt(1-MeCy(-H))]$_3$$^{3+}$ cation.

Table 5. Selected Bond Lengths (Å) and Angles (deg) for **2B**·2H$_2$O

Pt(1)–P(1)	2.262(5)	Pt(2)–N(3a)	2.12(1)
Pt(1)–P(2)	2.268(4)	N(3a)–C(4a)	1.41(2)
Pt(1)–N(3)	2.11(1)	N(4a)–C(4a)	1.26(2)
Pt(1)–N(4b)	2.08(1)	Pt(3)–P(5)	2.270(5)
N(3)–C(4)	1.39(2)	Pt(3)–P(6)	2.252(4)
N(4)–C(4)	1.30(1)	Pt(3)–N(4a)	2.10(1)
Pt(2)–P(3)	2.265(5)	Pt(3)–N(3b)	2.10(1)
Pt(2)–P(4)	2.261(4)	N(3b)–C(4b)	1.40(2)
Pt(2)–N(4)	2.10(1)	N(4b)–C(4b)	1.30(2)

P(1)–Pt(1)–P(2)	95.2(2)	P(3)–Pt(2)–N(3a)	90.2(4)
N(3a)–Pt(2)–N(4)	86.3(4)	P(4)–Pt(2)–N(4)	88.7(3)
P(1)–Pt(1)–N(3)	169.7(3)	Pt(2)–N(3a)–C(4a)	120.9(8)
P(2)–Pt(1)–N(4b)	170.4(3)	Pt(1)–N(4b)–C(4b)	128.4(8)
P(1)–Pt(1)–N(4b)	87.0(4)	N(3b)–C(4b)–N(4b)	120(1)
P(2)–Pt(1)–N(3)	90.8(3)	P(3)–Pt(2)–P(4)	94.9(2)
Pt(1)–N(3)–C(4)	125.0(7)	N(3b)–Pt(3)–N(4a)	86.9(4)
Pt(2)–N(4)–C(4)	124.4(9)	P(5)–Pt(3)–N(4a)	173.7(3)
N(3a)–C(4a)–N(4a)	120(1)	P(6)–Pt(3)–N(3b)	170.7(3)
N(3)–Pt(1)–N(4b)	88.4(4)	P(5)–Pt(3)–N(3b)	90.6(3)
P(5)–Pt(3)–P(6)	95.7(2)	P(6)–Pt(3)–N(4a)	87.5(3)
P(3)–Pt(2)–N(4)	176.1(3)	Pt(3)–N(3b)–C(4b)	124.5(8)
P(4)–Pt(2)–N(3a)	173.9(3)	N(3)–C(4)–N(4)	121(1)

The entire set of these spectroscopic data originally suggested to us the hypothesis that **2A** was a *mononuclear* complex, *cis*-[(PMe$_3$)$_2$Pt(1-MeCy(-H))](NO$_3$), in which the cytosinate ion acts as chelating ligand through the N(3) and N(4) donor atoms.[5] However, the X-ray analysis, carried out for the nitrate and perchlorate derivatives, has now proved that, in fact, the new complex is a *trinuclear* species in which the *cis*-(PMe$_3$)$_2$Pt units are symmetrically bridged by the cytosinate ligands.

Solid-State Structure of *cis*-[(PMe$_3$)$_2$Pt(1-MeCy(-H))]$_3$(ClO$_4$)$_3$·2H$_2$O, 2B·2H$_2$O. Figure 1 illustrates the molecular geometry and the labeling scheme of the cationic complex *cis*-[(PMe$_3$)$_2$Pt(1-MeCy(-H))]$_3$$^{3+}$ found both in the nitrate (**2A**) and perchlorate salts (**2B**). Table 5 lists selected bond lengths and angles observed for **2B**·2H$_2$O, for which better structural data were obtained. The trimeric cation *cis*-[(PMe$_3$)$_2$Pt(1-MeCy(-H))]$_3$$^{3+}$ contains three *cis*-(PMe$_3$)$_2$Pt units symmetrically bridged by the cytosinate anions through the N(3) and N(4) atoms. The resulting (Pt–N–C–N)$_3$ 12-membered ring has approximate S_3 symmetry. Each platinum atom is in a distorted square-planar arrangement in which the donor atoms are as follows: (a) the phosphorus atom of the two trimethylphosphines [(Pt–P = 2.263(5) Å (average); P–Pt–P = 95.1(1)° (average)], (b) the endocyclic N(3) [Pt–N(3) = 2.11(1) Å (average)], and (c) the exocyclic N(4) [Pt–N(4) = 2.09(1) Å (average)] atoms, respectively, of two bridging monoanionic 1-MeCy(-H) ligands [N(3)–Pt–N(4) = 87.2° (average)]. The donor atoms deviate substantially from the best P$_2$N$_2$ mean plane, mainly around Pt(1) and Pt(3) (up to –0.19 Å for N(4b) and to +0.13 Å for N(3b)), with the Pt atoms out by only 0.01 Å. The platinum atoms lie at the corners of a virtually equilateral triangle (mean Pt···Pt separation of 5.31 Å with mean Pt···Pt···Pt angle of 60°). The three nucleobase mean planes are inclined at angles of 56.2, 67.6, and 68.1° to the plane of the triangle defined by the Pt atoms. The differences in inclination are consistent with the slightly different Pt···Pt separations. The nucleobases are strictly planar, their centroids are equally placed far from the center of the triangle (*ca.* 3.8 Å), and the plane of the centroids is pratically parallel (dihedral angle of 4.1°) to that of Pt atoms, at a distance of 2.52 Å. Moreover, the three nucleobases are inclined toward each other (at a dihedral angle of *ca.* 102°) and the cation may be regarded as basin-shaped (Figure 2).

The C(1), C(1a), and C(1b) atoms form a triangle, which, in this description, is the rim of the basin; it lies above the two triangles formed by the three Pt atoms and the three centroids of the bases and is approximately (dihedral angles of 5.2 and 1.6°, respectively) parallel to them. In the crystal the tripositive cation and the ClO$_4^-$ counteranions are well-separated, while the two water molecules show weak interactions with the O(2) and O(2a) atoms. In particular, the Ow(2) atom is H-bonded to Ow(1) (at 2.77 Å) and to O(2a) (at x, $1 - y$, $1 - z$) (separation of 2.71 Å). On the other hand Ow(1) is located 2.82 Å from O(2) atom (see Figure B of the supplementary material).

The comparison of the bond distances and angles within the dinuclear (**1A**)[5] and trinuclear (**2B**) complexes does not show significant changes, with two major exceptions: (i) a decrease of the Pt–N(4)–C(4) angles which are found in the range 124(4)–128(4)° in **2B** and 136.4(7)–135.7(7)° in **1A**; (ii) an increase of the N(3)–Pt–N(4) angles, from an averaged value of 84.7(4)° in **1A** to 87.2(4)°. Thus, the increase of the Pt···Pt distance (from 2.199(2) Å in **1A** to 5.31 Å (average) in **2B**) allows to the ligands to assume a more regular square-planar arrangement around the metal center as indicated by the smaller deviation of the platinum from the mean plane passing through the four donor atoms (0.185 Å in **1A**, 0.01 Å (average) in **2B**).

Natural-Abundance ^{15}N NMR Investigations. The involvement of the N(3) and N(4) atoms of the cytosine ligands on platinum binding in both the dinuclear and trinuclear complexes has been confirmed in solution through a ^{15}N NMR study by obtaining the spectra at natural abundance. Although the use of a high-field magnet required for measurements of nuclei in very low isotopic abundance (^{15}N 0.37%) frequently precludes the observation of direct ^{195}Pt–^{15}N coupling constants,[15] the detection of the $^2J_{^{31}P-^{15}N}$ couplings can provide conclusive evidence about the stereochemistry and the nature of the donor atoms of the

---

(15) (a) Lallemand, J. Y.; Soulié, J.; Chottard, J. C.; *J. Chem. Soc., Chem. Commun.* **1980**, 436. (b) Pregosin, P. S. *Coord. Chem. Rev.* **1982**, *44*, 247. (c) Sparks, S.W.; Ellis, P. D. *J. Am. Chem. Soc.* **1986**, *108*, 3215.

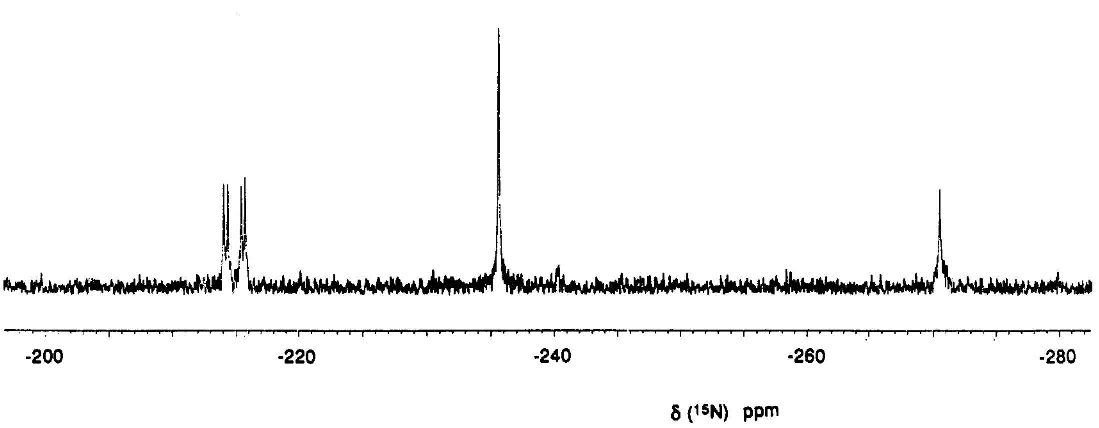

Figure 3. Natural-abundance $^{15}N\{^1H\}$ NMR spectrum of *cis*-[$(PMe_3)_2Pt(1\text{-}MeCy)_2](NO_3)_2$ (*ca* 0.5 M) in DMSO-d_6 solution. The spectrum was obtained with a modified INEPT procedure[11] by using a spectral width of 20 kHz, with 32 K data points, a relaxation delay of 2 s, and number of scans 5000. Typical parameters for the INEPT sequence were ^1H $P_w(90°) = 22$ μs and ^{15}N $P_w(90°) = 17$ μs; the utilized delay was calculated for a long-range coupling constant N–H = 8 Hz. The low intensity of the signal at –270.5 ppm is due to the specific sequence used, which was optimized for nitrogen atoms not bearing hydrogen.

complexes in solution. The magnitude of this coupling is known to be dependent on whether the two atoms are *cis* or *trans* to one another.[16] The observed values in a number of thiocyanate complexes $(PR_3)_2Pt(NCS)_2$ are in the range 50–70 Hz for the *trans* geometry and 10 Hz or less for the *cis* orientation. We have verified the validity of this criterion for structural assignments, obtaining at first the ^{15}N NMR spectrum of the mononuclear complex *cis*-[$(PMe_3)_2Pt(1\text{-}MeCy)_2](NO_3)_2$ in which the two *neutral* cytosine ligands are N(3)-bonded. In this compound, only the N(3) nitrogen is expected to exhibit $^2J_{^{31}P-^{15}N}$ interactions, and the pertinent spectrum is reported in Figure 3. The resonance centered at δ –214.9 occurs as a first-order multiplet with $^2J_{PN} = 54.9$ and 12.9 Hz owing to the coupling with the *trans* and *cis* phosphine ligands, respectively, and therefore is attributable to the N(3) atom. No coupling with the platinum atom is detectable, presumably as a consequence of the large contribution of the chemical shift anisotropy effect of the ^{195}Pt nuclei.[15]

The resonance at δ –270.5 was assigned to the N(4) atom through a two-dimensional ^1H–^{15}N shift correlation experiment and the pertinent spectrum is reported in Figure 4. As earlier observed,[2e] in the conventional ^1H NMR spectrum of *cis*-[$(PMe_3)_2Pt(1\text{-}MeCy)_2]^{2+}$ the cytosine NH_2 protons appear chemically unequivalent due to the hindered rotation of the NH_2 group.[7] Accordingly, in the F_2 axis of Figure 4 (proton projection) both the singlets, centered at 8.81 and 7.71 ppm, respectively, are attributable to hydrogen atoms bound to the same nitrogen as indicated by the single resonance observed in the corresponding ^{15}N projection (F_1 axis).

In Table 6 are collected the ^{15}N NMR data of the complex *cis*-[$(PMe_3)_2Pt(1\text{-}MeCy)_2](NO_3)_2$ and those of the free nucleobase.[17] From the chemical shift values of the free and platinated cytosine appears a remarkable upfield shift of the N(3) renonance upon coordination (54 ppm) and a less evident shift in the opposite direction for the exocyclic nitrogen resonance. The change of the ^{15}N chemical shift on metal coordination or protonation is usually ascribed to changes in the paramagnetic contribution to the nitrogen screening constant.[18] Similar variational trends of the chemical shifts for metal-bonded nitrogens in platinum(II)-nucleosides complexes have been also noticed.[19]

The ^{15}N NMR spectra of the complexes **1A** and **2A** are reported in Figure 5 and the pertinent data are collected in Table 6. Figure 5A refers to a 0.5 M solution of *cis*-[$(PMe_3)_2Pt(1\text{-}MeCy(\text{-}H))]_2(NO_3)_2$ in DMSO-d_6 containing *ca* 5% of *cis*-[$(PMe_3)_2Pt(1\text{-}MeCy(\text{-}H))]_3(NO_3)_3$. In contrast, Figure 5B refers to the same solution, after warming at 80 °C for 24 h, in which the content of the trinuclear species, on the basis of its ^{31}P NMR spectrum was *ca.* 45%. The spectrum of the dinuclear species is characterized by two doublets centered at –222.9 and –251.1 ppm attributable to the platinated nitrogen atoms N(3) and N(4), respectively. The assignment of the resonance at –251.1 ppm to the N(4) atom was achieved through an inverse detection experiment and the corresponding spectrum is reported in Figure 6. As seen in the F_2 axis of Figure 6, the resonance centered at δ 6.97 occurs as a doublet of doublets owing to the coupling of the N(4)H proton with the nitrogen atom ($^1J_{H-N} = -76.7$ Hz) and one of the phosphine ligands ($^3J_{H-P} = ca.$ 2 Hz). The remaining singlet at δ –246.8 of Figure 5A has to be attributed to the N(1) resonance.

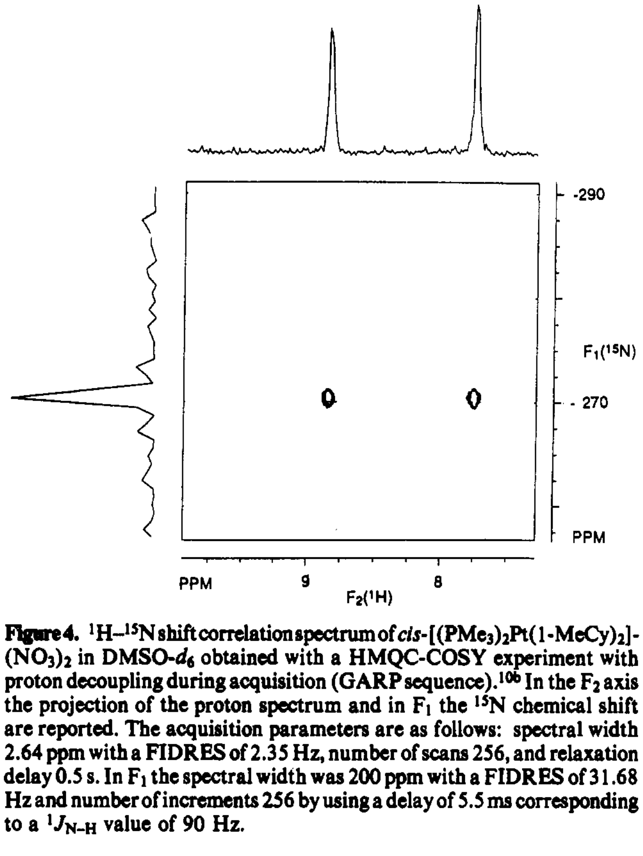

Figure 4. ^1H–^{15}N shift correlation spectrum of *cis*-[$(PMe_3)_2Pt(1\text{-}MeCy)_2](NO_3)_2$ in DMSO-d_6 obtained with a HMQC-COSY experiment with proton decoupling during acquisition (GARP sequence).[10b] In the F_2 axis the projection of the proton spectrum and in F_1 the ^{15}N chemical shift are reported. The acquisition parameters are as follows: spectral width 2.64 ppm with a FIDRES of 2.35 Hz, number of scans 256, and relaxation delay 0.5 s. In F_1 the spectral width was 200 ppm with a FIDRES of 31.68 Hz and number of increments 256 by using a delay of 5.5 ms corresponding to a $^1J_{N-H}$ value of 90 Hz.

From Figure 5 it is clear that the dinuclear and trinucler complexes exhibit very similar ^{15}N NMR spectra. The most

---

(16) Motchi, H.; Pregosin, P. S.; Venanzi, L. M. *Helv. Chim. Acta* **1979**, *62*, 667.
(17) Levy, G. C.; Lichter, R. L. In *Nitrogen-15 Nuclear Magnetic Resonance Spectroscopy*; John Wiley and Sons: New York, 1979; p 204.
(18) Markowski, V.; Sullivan, G. R.; Roberts, J. D. *J. Am. Chem. Soc.* **1977**, *99*, 714.
(19) (a) Nee, M.; Roberts, J. D. *Biochem.* **1982**, *21*, 4920. (b) Barbarella, G.; Bertoluzza, A.; Morelli, M. A.; Tosi, M. R.; Tugnoli, V. *Gazz. Chim. Ital.* **1988**, *118*, 637.

Table 6. ^{15}N NMR Data for Free and Coordinated 1-Methylcytosine–Platinum(II) Complexes (L = PMe$_3$) in DMSO-d_6

compd	δ(N$_1$)	δ(N$_3$) [$^2J_{N-P}$, Hz]	δ(N$_4$) [$^2J_{N-P}$, Hz]	δ(NO$_3^-$)
cis-[L$_2$Pt(1-MeCy(-H))]$_2$(NO$_3$)$_2$	–246.8 (s)	–222.9 (d) [44.9]	–251.1 (d) [46.9]	–0.2
cis-[L$_2$Pt(1-MeCy(-H))]$_3$(NO$_3$)$_3$	–246.1 (s)	–222.9 (d) [44.9]	–252.5 (d, d) [50.7, 2.4]	–0.2
cis-[L$_2$Pt(1-MeCy)$_2$](NO$_3$)$_2$	–235.6 (s)	–214.9 (d, d) [54.9, 12.9]	–270.5 (s)	–0.2
1-MeCy[a]	–224.1	–168.1	–283.0	

[a] Data from ref 17.

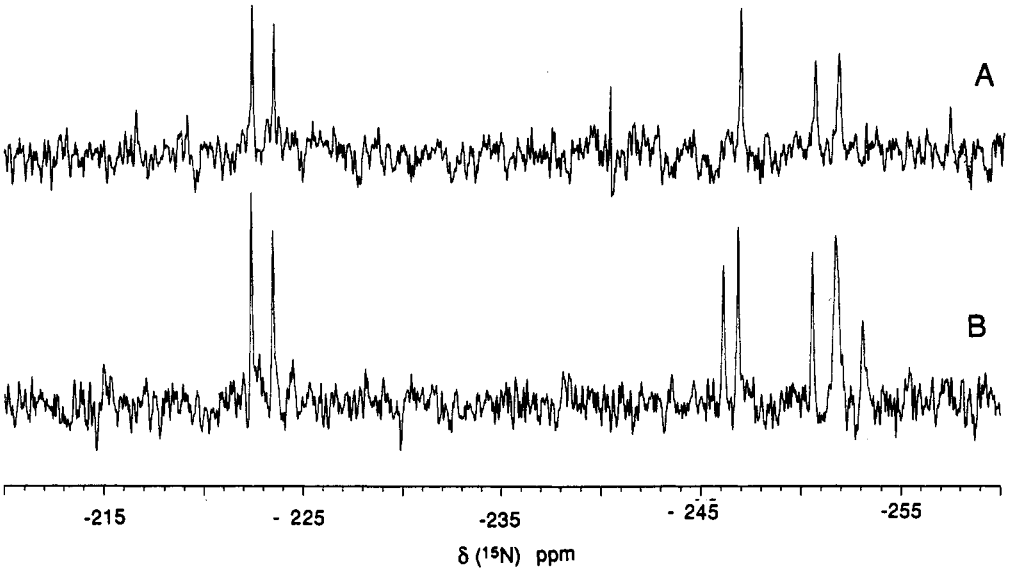

Figure 5. Natural-abundance ^{15}N{^{1}H} NMR spectrum of: (A) *cis*-[(PMe$_3$)$_2$Pt(1-MeCy(-H))]$_2$(NO$_3$)$_2$ and (B) a mixture of *cis*-[(PMe$_3$)$_2$Pt(1-MeCy(-H))]$_2$(NO$_3$)$_2$ and *cis*-[(PMe$_3$)$_2$Pt(1-MeCy(-H))]$_3$(NO$_3$)$_3$ in DMSO-d_6 solution. The spectrum was obtained with a modified INEPT procedure[11] by using a spectral width of 20 kHz, with 32 K data points, a relaxation delay of 2 s, and number of scans 5000. Typical parameters for the INEPT sequence were ^{1}H $P_w(90°)$ = 22 μs and ^{15}N $P_w(90°)$ = 17 μs; the utilized delay was calculated for a long range coupling constant N–H = 8 Hz. The low intensity of the signal at –270.5 ppm is due to the specific sequence used, which was optimized for nitrogen atoms not bearing hydrogen.

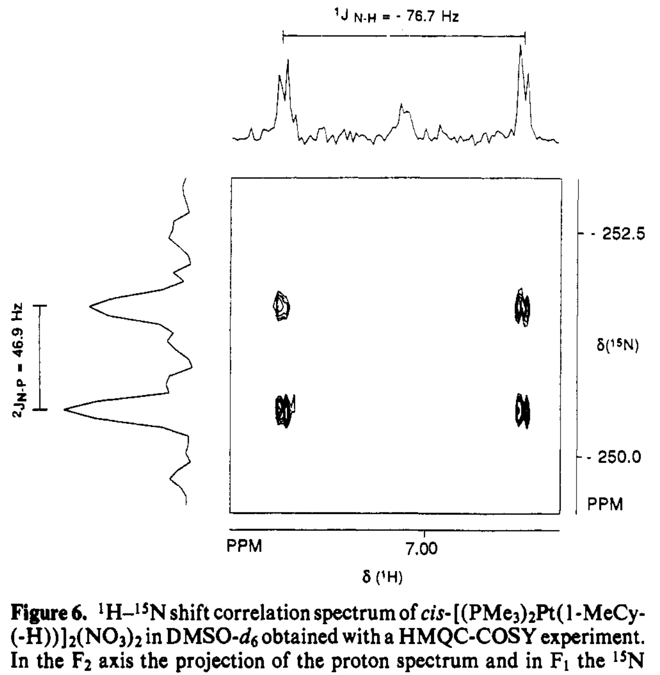

Figure 6. ^{1}H–^{15}N shift correlation spectrum of *cis*-[(PMe$_3$)$_2$Pt(1-MeCy(-H))]$_2$(NO$_3$)$_2$ in DMSO-d_6 obtained with a HMQC-COSY experiment. In the F$_2$ axis the projection of the proton spectrum and in F$_1$ the ^{15}N chemical shift are reported. The acquisition parameters are as follows: spectral width 2.64 ppm with a FIDRES of 2.35 Hz, number of scans 256, and relaxation delay 0.5 s. In F$_1$ the spectral width was 200 ppm with a FIDRES of 31.68 Hz and number of increments 256 by using a delay of 5.5 ms corresponding to a $^1J_{N-H}$ value of 90 Hz.

significant change of the spectroscopic parameters is seen for the N(4) resonance which appears shifted 1.4 ppm upfield in the trinuclear species, with a concomitant increase of both the ^{15}N–^{31}P coupling constants. In fact, whereas in **1A** the N(4) nucleus appears coupled only with the phosphorus atom in a mutually *trans* position ($^2J_{N-P}$ = 46.9 Hz), in **2A** N(4) is coupled with the P atoms in mutually *trans* and *cis* positions with $^2J_{N-P}$ = 50.7 and 2.4 Hz, respectively. The endocyclic N(3) nitrogen shows the same values of chemical shift and $^2J_{N-P}$ in the two complexes, indicating that it is mainly the exocyclic nitrogen which is involved in a partial reorganization of its electronic distribution when the trinuclear species is formed. This result is in agreement with the structural data obtained in the solid state. Although the Pt–N(4) bond distances are only slightly changed [in the range 2.08(1)–2.10(1) Å in **2B** and 2.058(8)–2.074(8) Å in **1A**], the Pt–N(4)–C(4) angles undergo a remarkable decrease in the trinuclear complex, approaching the value expected for a regular sp^2 hybrid on the N(4) atom.

The comparison of the ^{15}N NMR data of **1A** and **2A** with those of *cis*-[(PMe$_3$)$_2$Pt(1-MeCy)$_2$]$^{2+}$ (Table 6) indicates that the deprotonation of the nucleobase at the NH$_2$ position determines a charge redistribution within the entire pyrimidinic ring as indicated by the variation of *all* of the nitrogen resonances. In particular, the exocyclic N(4) atom of the nucleobase in **1A** and **2A** appears remarkably deshielded (18–19 ppm) in comparison with the corresponding resonance in *cis*-[(PMe$_3$)$_2$Pt(1-MeCy)$_2$](NO$_3$)$_2$.

Conclusions

Unlike the ammino complex *cis*-[(NH$_3$)$_2$Pt(1-MeCy(-H))]$_2^{2+}$, the trimethylphosphino analogue **1** rearranges to the trinuclear species **2** characterized by a high thermodynamic stability. In fact, the reaction can be carried out in aqueous solution at 100 °C without significant decomposition of the reaction product. The driving force for the oligomerization reaction has to be related to a more favorable metal-ligand interaction in the trinuclear species, likely due to the lower *intramolecular* repulsion of the *cis*-(PMe$_3$)$_2$Pt moieties. Although the structural data do not show significant differences of the platinum-phosphorus bond distances and angles in the two complexes, the shift at lower field of the ^{31}P NMR resonance observed in **2**, for both phosphine ligands, is a clear indication of a stronger interaction of these ligands with the metal center. The upfield shift (1.4 ppm) and the higher values of $^2J(^{15}N-^{31}P)$ of the N(4) resonance found in the ^{15}N NMR spectrum of the trinuclear species also appears to be in line with this conclusion. Finally, it is worth noticing that the formation of a twelve-menbered ring causes an upfield shift of the ^{195}Pt NMR resonance which is in agreement with that observed for similar rearrangements in a number of hydroxo-bridged platinum complexes.[20]

Interestingly enough, the same reaction is not observed in the case of the related complex *cis*-$[(PMe_3)_2Pt(9\text{-}EtAd(\text{-}H))]_2(NO_3)_2$. The 9-methyladenine derivative, containing the N(6)-deprotonated nucleobase, has structural features similar to those of **1**, *i.e.* the same head-to-tail conformation of the nucleobases and the presence of an eight membered Pt_2N_4-ring.[6] The reaction mixture resulting from the reaction of *cis*-$[(PMe_3)_2Pt(\mu\text{-}OH)]_2(NO_3)_2$ with 9-methyladenine shows, in addition to the dinuclear species, the presence of a small amount (< 5%) of a second species whose spectroscopic data (^{31}P NMR) could be consistent with the formation of a trinuclear derivative. However, in the same conditions in which the conversion of **1** to **2** occurs quantitatively, the complex *cis*-$[(PMe_3)_2Pt(9\text{-}EtAd(\text{-}H))]_2(NO_3)_2$, appears unchanged.

Acknowledgment. Parke-Davis is gratefully acknowledged for a research grant to G.T.. We thank Progetto Finalizzato Chimica Fine II, C.N.R., for partial financial support.

Supplementary Material Available: Tables of complete crystallographic data, bond lengths and angles, and anisotropic thermal parameters for **2B**·$2H_2O$, and figures showing the superposition of the cation *cis*-$[(PMe_3)_2Pt(1\text{-}MeCy(\text{-}H))]_3^{3+}$ in **2A**·EtOH·H_2O and **2B**·$2H_2O$ and a packing diagram for **2B**·$2H_2O$ (6 pages). Ordering information is given on any current masthead page.

---

(20) Rochon, F. D.; Melanson, R.; Morneau, A. *J. Magn. Reson. Chem.* **1992**, *30*, 697.